HHS Public Access

Author manuscript

Nature. Author manuscript; available in PMC 2014 October 03.

Published in final edited form as:

Nature. 2014 April 3; 508(7494): 88–92. doi:10.1038/nature13028.

The hippocampal CA2 region is essential for social memory

Frederick L. Hitti[1] and **Steven A. Siegelbaum**[1,2]

[1]Department of Neuroscience, Kavli Institute, Howard Hughes Medical Institute, College of Physicians and Surgeons, Columbia University 1051 Riverside Dr. New York, NY 10032

[2]Department of Pharmacology, Kavli Institute, Howard Hughes Medical Institute, College of Physicians and Surgeons, Columbia University 1051 Riverside Dr. New York, NY 10032

Summary

The hippocampus is critical for encoding declarative memory, our repository of knowledge of who, what, where, and when[1]. Mnemonic information is processed in the hippocampus through several parallel routes involving distinct subregions. In the classic trisynaptic pathway, information proceeds from entorhinal cortex (EC) to dentate gyrus (DG) to CA3 and then to CA1, the main hippocampal output[2]. Genetic lesions of EC[3] and hippocampal DG[4], CA3[5], and CA1[6] regions have revealed their distinct functions in learning and memory. In contrast, little is known about the role of CA2, a relatively small area interposed between CA3 and CA1 that forms the nexus of a powerful disynaptic circuit linking EC input with CA1 output[7]. Here, we report a novel transgenic mouse line that enabled us to selectively examine the synaptic connections and behavioral role of the CA2 region in adult mice. Genetically targeted inactivation of CA2 pyramidal neurons caused a pronounced loss of social memory, the ability of an animal to remember a conspecific, with no change in sociability or several other hippocampal-dependent behaviors, including spatial and contextual memory. These behavioral and anatomical results thus reveal CA2 as a critical hub of sociocognitive memory processing.

Although the CA2 region was first described by Lorente de Nó in 1934[8] relatively little is known about its functional properties and behavioral role. To examine the importance of this region, we generated a transgenic mouse line (*Amigo2-Cre*) that expresses Cre recombinase predominantly in CA2 pyramidal neurons (PNs) in adult mice (Extended Data Fig. 1). Because this line expresses Cre throughout the brain during early development, as well as in certain limited areas outside of CA2 in the adult, we stereotactically injected Cre-dependent adeno-associated virus (AAV) into the hippocampus of adult *Amigo2-Cre* mice to limit viral expression to CA2 pyramidal cells.

Address correspondence to: sas8@columbia.edu.

Author Contributions F.L.H planned and performed the experiments, analyzed the data, and wrote the manuscript. S.A.S oversaw the overall execution of the project, contributed to the experimental design and the interpretation of the data, provided financial support, and helped write the manuscript.

The authors declare no competing interests.

To determine the specificity of CA2 expression in the transgenic line, we bilaterally injected into dorsal hippocampus a Cre-dependent AAV to express yellow fluorescent protein (YFP) in Cre^+ cells (Fig. 1a). We observed selective and robust YFP expression in CA2 PNs throughout dorsal hippocampus[9-11] (Fig. 1b; Extended Data Fig. 2a). We confirmed that the Cre^+ cells were indeed CA2 PNs by demonstrating co-staining for RGS14[12] (97.38 ± 0.31% overlap; n = 4 mice, 2546 cells; Fig. 1c-e and Extended Data Fig. 3) and other known CA2 PN markers (Extended Data Fig. 2). In contrast, there was no co-staining for a CA1 PN marker (Extended Data Fig. 2). Additionally, the electrophysiological properties of the YFP^+ neurons differed significantly from those of CA1 PNs (Extended Data Table 1) and largely matched the values previously reported for CA2 pyramidal neurons[7]. Only a minute fraction of YFP^+ neurons were also $GABA^+$ (0.16 ± 0.16%; n = 3 mice, 1539 cells), demonstrating the specific targeting of CA2 excitatory PNs (Fig. 1f, g and Extended Data Fig. 3). Finally, our AAV injections resulted in the targeting of the vast majority of CA2 PNs in the dorsal hippocampus, measured by the percentage of $RGS14^+$ cells that were also YFP^+ (82.33 ± 2.37%, n = 4 mice, 2992 cells).

Next, we mapped CA2 synaptic input and output using viral tracing strategies that take advantage of the genetic targeting of CA2 PNs in the *Amigo2-Cre* mice, and largely confirmed results of previous studies using conventional[13] and genetic-based[14] approaches. Monosynaptic inputs to CA2 PNs were determined using an EnvA pseudotyped ΔG rabies virus strategy[15] (Extended Data Fig. 4). Unilateral viral injections revealed bilateral inputs from CA3 and CA2 (Fig. 2a, b) and strong unilateral input from both lateral and medial EC layer II neurons (Fig. 2c, d). In addition, synaptic inputs were detected from medial septum and diagonal band (Fig. 2e), median raphe nucleus (Fig. 2f), and the supramammillary nucleus of the hypothalamus (Fig. 2g).

Surprisingly, we observed only sparse labeling of EC layer III neurons with the rabies virus approach. Our laboratory previously concluded that EC LIII axons provide strong excitatory drive to CA2 PNs, based on the finding that large excitatory postsynaptic potentials (EPSPs) are evoked in CA2 PNs with a focal stimulating electrode placed in the stratum lacunosum (SLM) of the CA1 region[7], where axons from LIII EC neurons are thought to provide the predominant source of excitatory inputs. Our present results, combined with recent results[13,14] suggest that these synaptic responses recorded in CA2 PNs may result from activation of LII fibers that course through or near SLM in CA1.

Output projections from CA2 were determined by expressing YFP in CA2 PNs (as in Fig. 1) and examining brains for YFP fluorescent axons. Unilateral viral injections resulted in strong bilateral labeling in hippocampal CA1, CA2, and CA3 regions, with densest projections observed in stratum oriens (SO) and weaker projections detected in stratum radiatum (SR) (Fig. 2h, i). We did not observe extra-hippocampal outputs.

These anatomical results generally support previous[13,14] findings. However, we failed to observe vasopressinergic input to CA2 from the paraventricular nucleus of the hypothalamus[13], which may reflect an inability of the transsynaptic rabies tracing system to label peptidergic inputs[15]. We also did not observe CA2 output to the supramammillary nucleus[13], suggesting this output may represent an inhibitory projection from CA2 as we

selectively labeled PNs. Moreover, we did not observe CA2 output to EC layer II[16], perhaps because the anterograde tracing failed to detect weak connections.

To examine directly the functional and behavioral relevance of CA2, we employed the *Amigo2-Cre* mouse line to inactivate output from CA2 PNs selectively. We injected into the dorsal hippocampus of the *Amigo2-Cre* mice a Cre-dependent AAV to express tetanus neurotoxin (TeNT) light chain fused to green fluorescent protein (eGFP-TeNT) in CA2 PNs to block their synaptic output. We first verified the efficacy of this approach and characterized the influence of CA2 on its CA1 PN targets by co-expressing the light-activated cation channel channelrhodopsin-2 (ChR2)[17] with either TeNT or YFP using Cre-dependent AAVs. Low intensity illumination (using 2-ms pulses of 470 nm light at 3 $mW{\cdot}mm^{-2}$) focused on CA2 reliably triggered action potentials in CA2 PNs, as seen by the presence of fast action currents in cell-attached patch clamp recordings (Fig. 3a-c). Similar spiking was seen in neurons that co-expressed either YFP (Fig. 3b) or TeNT (Fig. 3c) with ChR2, indicating that the TeNT did not inhibit excitability.

Next, we determined the strength of synaptic transmission from CA2 to CA1 PNs using whole-cell current-clamp recordings to measure light-evoked postsynaptic potentials (PSPs) in CA1 PNs from hippocampal slices in which ChR2 and YFP were expressed in CA2 PNs (Fig. 3d). In agreement with anatomical mapping (Fig. 2h, i) and paired recordings[7], focal photostimulation delivered to CA1 SO and SR regions evoked robust monosynaptic PSPs (mean latency 1.22 ± 0.06 ms, n = 119 observations) in nearby CA1 PNs (Fig. 3e). Increasing the light intensity recruited progressively larger PSPs, presumably due to an increase in the number of optically-activated CA2 axons (Fig. 3e, f). In stark contrast, in slices in which TeNT was co-expressed with ChR2 in CA2 PNs, illumination over a wide range of intensities produced little or no synaptic response in CA1 neurons (Fig. 3e, f), demonstrating the efficacy of the TeNT lesion.

What are the behavioral consequences of inactivation of CA2? To address this question, we compared the behavior of control mice (CA2-YFP) with mice in which CA2 PNs were inactivated (CA2-TeNT), using viral injections in dorsal hippocampus[11]. Functional inactivation of dorsal CA2 did not alter locomotor activity or anxiety-like behavior (Extended Data Fig. 5). Surprisingly, CA2-inactivation also did not significantly alter hippocampal-dependent spatial memory assessed by the Morris water maze (although there was a trend for the CA2-inactivated mice to learn the task more slowly; Extended Data Fig. 6). Nor was there any change in hippocampal-dependent contextual fear memory or amygdala-dependent auditory fear memory (Extended Data Fig. 7).

The finding that CA2 PNs integrate synaptic input from lateral EC (which conveys non-spatial information[18]) with subcortical input from both the serotonergic median raphe nucleus[19] and the hypothalamic supramammillary nucleus[20] suggests a potential role for CA2 in non-spatial hippocampal tasks. Previous studies have shown that the mRNA for the vasopressin 1b receptor (*Avpr1b*) is strongly expressed in CA2[21] and that unconditional deletion of this gene impairs social recognition memory[22,23]. However, *Avpr1b* mRNA is also expressed outside hippocampus[21] and its deletion results in changes in non-hippocampal dependent behaviors, including reduced aggression and decreased

sociability[22,23], raising questions as to the selective role of CA2 in the knockout phenotype[24].

To assess directly the role of CA2 in social behavior, we first compared the performance of CA2-YFP versus CA2-TeNT mice in a three-chamber test of sociability[23], which examines the normal preference of a subject mouse for a chamber containing a littermate versus an empty chamber (Fig. 4a). In contrast to the effect of *Avpr1b* deletion, selective silencing of CA2 did not alter sociability as the CA2-TeNT and CA2-YFP groups displayed a significant and similar preference for the compartment containing the littermate (Fig. 4a).

In contrast to their normal sociability, CA2-TeNT mice displayed a profound deficit in social recognition as determined by a three-chamber social novelty test[23] (Fig. 4b). In this test, social recognition was measured by the increased time a subject mouse spent interacting with a novel unrelated mouse compared to the time it spent interacting with a familiar co-housed littermate. Multiple comparison testing revealed that the CA2-YFP control group demonstrated a significant preference for the compartment containing the novel animal whereas the CA2-TeNT group did not (Fig. 4b). Moreover, the difference score (time spent exploring the novel mouse minus time spent exploring the familiar mouse) of the CA2-TeNT group was significantly less than that of the CA2-YFP group (Fig. 4b). This deficit was not due to a lack of interest in novelty, *per se*, as the CA2-TeNT mice demonstrated normal preference for a novel object as assayed by two different novel object recognition protocols (Extended Data Fig. 8).

As the social novelty test does not incorporate a defined learning phase or delay period, we next conducted a more specific test of social memory, the direct interaction test[25]. For this test, a subject mouse was exposed to an unfamiliar mouse in trial 1. After a 1-h inter-trial interval (ITI), the subject mouse was either re-exposed to the same mouse encountered in trial 1 (Fig. 4c) or exposed to a second unfamiliar mouse (Fig. 4d). Social memory, measured as the decreased time a subject mouse spends exploring a previously encountered mouse, was fully suppressed by CA2 inactivation (Fig. 4c). In contrast, CA2 silencing did not alter sociability as evidenced by the equal exploration times for trials 1 and 2 when a subject mouse encountered two different unfamiliar mice in successive trials (Fig. 4d).

We next conducted a more stringent 5-trial social memory assay[26] to confirm that CA2-inactivation abolishes social memory. In this assay, a stimulus mouse was presented to a subject mouse for 4 successive trials. On the fifth trial, a novel stimulus mouse was introduced (Fig. 4e). The CA2-YFP control group of mice displayed normal social memory, as evidenced by a marked habituation (decreased exploration) during trials 1-4 and a striking dishabituation (increased exploration) upon presentation of a novel animal on the fifth trial. In contrast, the CA2-TeNT group showed no significant habituation during the four exposures to the stimulus mouse or dishabituation to the novel stimulus mouse, thus confirming the necessity of CA2 for social memory.

As olfaction is crucial for normal social interaction[27], we examined whether CA2 silencing influenced the detection or recognition of non-social or social odors. CA2-TeNT mice showed no loss in the ability to detect the presence of food buried under a deep layer of cage

bedding, a test of non-social odor detection (Extended Data Fig. 9a). Next, we used an olfactory habituation/dishabituation test (Extended Data Fig. 9b) and found that CA2 inactivation also had no effect on the ability of the mice to detect or discriminate either non-social or social odors. Thus, we conclude that the deficit in social memory in the CA2-TeNT mice was not due to a defect in sensing social or non-social odors.

Here, we developed and validated an *Amigo2-Cre* mouse line that enables precise genetic targeting of excitatory CA2 PNs, allowing us to map selectively the inputs and outputs of this largely unexplored region and demonstrate that the CA2 subfield is essential for social memory. Although we observed a fairly specific deficit in social memory following inactivation of dorsal CA2 pyramidal neurons, our results do not rule out the possibility that CA2 may participate more generally in hippocampal-dependent memory tasks. Thus, other regions of hippocampus may be able to compensate for loss of any role that CA2 may normally play in performance of the water maze or contextual fear conditioning tasks. Alternatively, CA2 may be selectively required for performance of more demanding non-social memory tasks.

The importance of human hippocampus for social memory is famously illustrated by the case of Henry Molaison (patient H.M.), who, following bilateral medial temporal lobe ablation, could not form new memories of people he had worked with for years[28]. Lesions limited to the hippocampus also impair social memory in both humans[1] and rodents[25]. As a number of neuropsychiatric disorders are associated with altered social endophenotypes, our findings raise the possibility that CA2 dysfunction may contribute to these behavioral changes. This possibility is supported by findings of a decreased number of CA2 inhibitory neurons in individuals with schizophrenia and bipolar disorder[29] and altered vasopressin signaling in autism[30]. Thus, CA2 may provide a novel target for therapeutic approaches to the treatment of social disorders.

Methods

Generation of *Amigo2-Cre* mouse line

Selective expression of *Amigo2* in the CA2 region of hippocampus was identified based on GENSAT[31] and Allen Brain Atlas[32] data. The RP23-288P18 bacterial artificial chromosome (BAC) that contained the *Amigo2* gene and its surrounding regulatory elements was obtained from the BACPAC Resource Center[33]. Recombineering with galK selection and the SW102 bacterial strain[34] was employed to seamlessly modify RP23-288P18 so that a Cre-HSV-polyA cassette was inserted at the translation start site of the *Amigo2* gene. Specifically, the Cre expression cassette was PCR amplified from pLD53.SC-Cre[35]. The homology arms used for the recombineering were 5' arm: 5’-ATTGGTGGGAGACTGAGCTGATGAGAAGCGACTGGCAAGAGACTCAGAGGCGACCATA-3’ and 3’ arm: 5’-ATGTCGTTAAGGTTCCACACACTGCCCACCCTGCCTAGAGCTGTCAAACCGGGTTGCAGAGA-3’. This modified BAC was injected into B6CBA/F2 pronuclei and embryos were implanted into pseudopregnant females. PCR was used to identify the offspring that were Cre-positive. These founders were crossed to the Ai14 Cre-reporter line[36] to examine the specificity of Cre expression. At 12 weeks of age, the Cre^+ offspring were transcardially

perfused with 4% paraformaldehyde (PFA) in phosphate buffered saline (PBS) and expression of tdTomato was examined in 50 μm coronal slices. CA2-specific expression of tdTomato was not observed in any of the founder lines. However, injection of the EF1α-FLEx-eYFP-WPRE-hGH Cre-reporter adeno-associated virus (AAV) into the hippocampus of adult mice (> 8 weeks old) revealed CA2-specific expression in 1 of the 6 founder lines. This line was used for all of the studies presented here. The line was backcrossed to C57BL/6J a minimum of 6 times before any behavioral or physiological experiments were performed.

Subjects

The *Amigo2-Cre* line was maintained as a hemizygous line on the C57BL/6J background by breeding Cre^+ males to C57BL/6J females. Only Cre^+ males were used for these experiments. Mice > 8 weeks old were injected with virus under stereotactic control into the hippocampus proper to avoid *Amigo2-Cre* expression in mossy cells of the dentate gyrus. All anatomical, behavioral, and physiological experiments were conducted 2-4 weeks following injection. All procedures were approved by the Institutional Animal Care and Use Committee at Columbia University and the New York State Psychiatric Institute.

Virus constructs

AAV5- EF1α-FLEx-eYFP-WPRE-hGH (4×10^{12} virus molecules ml^{-1}) was injected to label CA2 PNs and trace their axons. (EnvA)SAD-ΔG-mCherry (1×10^8 infectious particles ml^{-1}) pseudotyped rabies virus was produced as previously described[37] and used to label monosynaptic inputs to CA2. This virus can only infect cells expressing the TVA receptor[37,38]. Before rabies virus injection, AAV5- EF1α-FLEx-TVA-mCherry-WPRE-hGH[38] (3×10^{12} virus molecules ml^{-1}) was injected to express TVA in CA2. To permit retrograde synaptic transport of the ΔG virus, AAV5- CAG-FLEx-rabiesG-WPRE-hGH[38] (2×10^{12} virus molecules ml^{-1}) was co-injected with the TVA virus to express G in CA2. The aforementioned AAVs were obtained from the University of North Carolina vector core. To specifically excite CA2 PNs, AAV5-EF1α-FLEx-hChR2(H134R)-EYFP-WPRE-hGH (2×10^{12} genome copies ml^{-1}) was injected to express ChR2 in the CA2 neurons. This vector was obtained from the University of Pennsylvania (UPenn) vector core. To ablate CA2 pyramidal cell output, tetanus neurotoxin light chain (TeNT) was expressed selectively in these cells. A Cre-dependent AAV vector carrying eGFP-TeNT was created by PCR amplifying eGFP-TeNT from pTRE2-eGFP-TeNT-PEST[39] and subcloning it into pAAV-EF1α-DIO-hChR2-mCherry-WPRE (Addgene plasmid 20297) between the NheI and AscI sites in the inverse orientation. The resulting vector, pAAV- EF1α-FLEx-eGFP-TeNT-WPRE-hGH was sent to the UPenn vector core for custom production of AAV5- EF1α-FLEx-eGFP-TeNT-WPRE-hGH (1×10^{13} genome copies ml^{-1}).

Stereotaxic injection

Mice were anesthetized with isoflurane (2-5%) and placed in a stereotaxic apparatus (Digital Just for Mice Stereotaxic Instrument, Stoelting). The head was fixed, and the skull was exposed. Burr holes were made and a glass micropipette (Drummond Scientific) was slowly lowered into the dorsal hippocampus at −1.6 mm anteroposterior, ±1.6 mm mediolateral,

and −1.7 mm dorsoventral relative to bregma. The pipettes were formed with 20μm diameter tips using a P-2000 laser puller (Sutter Instrument). For the mouse line validation, anterograde tracing, and behavioral experiments, 180 nl of virus was pressure injected into each hemisphere. For the retrograde tracing experiments, 180 nl of a 1:5 mix of the TVA and rabies G AAV vectors was injected unilaterally. For the electrophysiological experiments, 360 nl of a 1:1 mix of ChR2 AAV and either YFP or TeNT AAV was injected. After injection, the pipette remained in place for 5min and then was slowly retracted. The mice were placed on a heating pad (TR-200, Fine Science Tools) throughout the duration of the surgery. Following injection, the scalp was sutured, saline was administered subcutaneously, and buprenorphine (0.05-0.1 mg/kg) was administered intraperitoneally for analgesia. The mice were placed under heating lamps during recovery from anesthesia. For the retrograde tracing experiments, these procedures were repeated two weeks after the initial AAV injection to inject 360 nl of (EnvA)SAD-ΔG-mCherry rabies virus. To test the specificity of the rabies virus, a subset of animals was injected with 360 nl of the (EnvA)SAD-ΔG-mCherry rabies virus without prior injection of AAVs expressing TVA and G. All injections were verified histologically. No injections were mistargeted, hence no subjects were excluded from analysis due to injection failure.

Immunohistochemistry and confocal microscopy

Mice were administered ketamine/xylazine (150 mg/kg, 10 mg/kg) and transcardially perfused with ice-cold PBS followed by ice-cold 4% PFA in PBS. Brains were postfixed overnight in 4% PFA in PBS and 50μm slices were prepared (Vibratome 3000 Plus, The Vibratome Company). Antigen retrieval[40] was performed for RGS14 staining. Briefly, free-floating sections were incubated at 80°C for 30 min in 50 mM sodium citrate (pH = 8.5). Slices were permeabilized with 0.2% Triton X-100 in PBS and blocked with 10% goat serum in PBS. The sections were incubated at 4°C overnight in primary antibody (1:50 dilution, NeuroMab, 73-170). For PCP4[10], STEP[41], WFS[42], and GABA staining, sections were permeabilized and blocked as above and then incubated in PCP4 (1:200 dilution, Sigma-Aldrich, HPA005792), STEP (1:500 dilution, Cell Signaling Technology, 4396), WFS1 (1:250 dilution, Proteintech, 11558-1-AP), or GABA (1:500 dilution, Sigma-Aldrich, A2052) primary antibodies at 4° C overnight. Sections were washed the following day and incubated for 2h with Alexa 555 or 647 secondary antibody (1:500 dilution, Invitrogen, A21422, A21428, or A21245) and NeuroTrace (1:250 dilution, Invitrogen, N21479 or N21483). Slices were then mounted with either Prolong Gold (Invitrogen, P36930) or VECTASHIELD (Vector Laboratories, H-1000) and imaged. An inverted laser scanning confocal microscope (LSM 700, Zeiss) was used for fluorescence imaging followed by analysis in ImageJ[43]. For cell counting experiments, every fifth slice throughout the rostral half of the hippocampus (5 slices in total) was examined. The first section was randomly chosen, and cells were assessed for double labeling in a single optical section taken near the middle of the slice.

Electrophysiology

2-3 weeks following AAV injection, mice were anesthetized with isoflurane (5%) and transcardially perfused with an ice-cold dissection solution that contained (in mM): 10 NaCl, 195 sucrose, 2.5 KCl, 10 glucose, 25 $NaHCO_3$, 1.25 NaH_2PO_4, 2 Na Pyruvate, 0.5 $CaCl_2$

and 7 $MgCl_2$. The hippocampi were dissected out and 400-μm thick slices were cut (VT1200S, Leica) perpendicular to the longitudinal axis of the hippocampus. The slices were then transferred to a chamber containing a 1:1 mixture of dissection solution and artificial cerebrospinal fluid (aCSF). The aCSF contained (in mM): 125 NaCl, 2.5 KCl, 22.5 glucose, 25 $NaHCO_3$, 1.25 NaH_2PO_4, 3 Na Pyruvate, 1 Ascorbic Acid, 2 $CaCl_2$ and 1 $MgCl_2$. Slices were incubated at 30°C for 30 min and then at room temperature for at least 1.5 hr before recording. Slices were transferred to a recording chamber (Warner Instruments), perfused with aCSF, and maintained at 33° C. All solutions were saturated with carbogen (95% O_2 and 5% CO_2). Whole-cell recordings were obtained from PNs with a patch pipette (3–5 MΩ) containing (in mM): 135 $KMeSO_4$, 5 KCl, 0.1 EGTA-Na, 10 HEPES, 2 NaCl, 5 ATP, 0.4 GTP, 10 phosphocreatine at pH 7.2 and osmolarity of 280–290 mOsm. Series resistance, which was always less than 30 MΩ, was monitored and compensated throughout the experiment. Cells with a 15% or greater change in series resistance were excluded from analysis. To activate ChR2, 2 ms pulses of blue (470 nm) light (M470L2-C1, Thor Labs) were delivered through a 20X objective. Light power from the objective was measured with a power meter (PM100D, Thor Labs). The objective was centered on the neuron that was being recorded during the experiment. For the CA2 cell-attached recordings, a gigaohm seal was made and action currents were measured in voltage-clamp mode (cell clamped at −70 mV) while 5 pulses of blue light were delivered. For the input-output curves, whole-cell recordings were made from CA1 PNs in current-clamp mode and the objective was centered on the patched CA1 neuron. This provided illumination over stratum oriens (SO), stratum pyramidale (SP), and stratum radiatum (SR) thus activating the CA2 projections to CA1 that course through SO and SR.

Behavioral tests

Mice were housed 2-5 per cage and were given *ad lib* access to food and water. They were kept on a 12 h (6 A.M. to 6 P.M.) light–dark cycle in a room maintained at 21°C. All tests were conducted during the light cycle. Mice were habituated to handling and transport from the colony room to the behavioral room for 3 days before behavioral tests were begun. Mice were given 1 h to habituate after transport to the behavioral room before any tests were conducted. The experimenter was blind to the treatment groups. The control group (CA2-YFP) was injected with AAV5- EF1α-FLEx-eYFP-WPRE-hGH while the CA2-inactivated group (CA2-TeNT) was injected with AAV5- EF1α-FLEx-eGFP-TeNT-WPRE-hGH. To blind the experimenter and randomize the treatment groups, virus aliquots were stored as pairs of coded cryotubes. Half of the mice in each home cage were injected with the YFP virus, while the other half were injected with the TeNT virus. The identity of the groups was revealed only after testing was completed. For the elevated plus maze, novel object, Morris water maze, and 3-chamber tests, mice were tracked with an overhead FireWire camera (DMK 31AF03-Z2, The Imaging Source) and ANY-maze (Stoelting). Freezing during fear conditioning was tracked with a Fire-i (Unibrain) camera and analyzed with ANY-maze (Stoelting). All apparatuses and testing chambers were cleaned with 70% isopropanol wipes (VWR) between animals unless otherwise indicated below.

Open field

Mice were placed in an open field (ENV-510S, Med Associates, Inc.) for 30 min and locomotor and rearing activity was monitored via IR beam breaks and recorded by the Activity Monitor (Med Associates, Inc.) software. The entire apparatus was enclosed in a sound attenuating cubicle.

Elevated plus maze

Mice were placed in the center of a maze (Stoelting) constructed in the shape of a plus with two enclosed arms (15 cm high walls) and two open arms. The maze was elevated 40 cm from the ground. Mice were allowed to explore the maze for 8 min. Entry into an arm was scored only after 85% of the animal's tracked body area was in the arm.

Novel object

Two variations of the novel object task were run. Both were conducted in a 50 cm long × 25 cm wide × 30.5 cm high arena. For both tests, the snouts of the mice were tracked and object interaction was measured as time spent with snout within 2 cm of the object. The objects (a glass chess piece, a small metal lock, and a small plastic box) were secured to the arena with neodymium magnets to render them immovable. In the first variation, mice were habituated to the arena and objects 1 and 2 over the course of four 5 min trials separated by an ITI of 10 min. Mice were then tested for object recognition memory 1 h after the fourth trial during the 5 min-long fifth trial. Either object 1 or object 2 (counterbalanced) was swapped for object 3 during the fifth trial. In the second variation of this test, the mice were habituated to the empty arena for 10min each day for 3 consecutive days. On day 4, the mice were exposed to a pair of either object 1 or object 2 for 5 min. Object recognition memory was tested 1 h after this trial by exposure to objects 1 and 2 for 5 min. In both protocols, object recognition memory was measured as the increased time spent investigating the novel object.

Morris water maze

The Morris water maze task was run over the course of 14 days in a 120 cm diameter pool filled with water that was opacified with non-toxic white paint (Prang tempera paint, VWR). The water was maintained at 19-20° C. Four 1 min trials were administered per day, and mice were run in groups of 8. On days 1-2, cued learning was conducted. During this procedure, mice were trained to find a circular platform (10cm in diameter) submerged 1 cm below the surface of the water and marked with a flag. Distal cues in the room were obscured by a black curtain that encircled the tank. The mouse was removed from the tank and returned to its home cage 15s after locating the platform. If a mouse failed to locate the platform during the minute-long trial, it was gently guided towards the platform. The mice were released from different start points at the beginning of each trial, and the platform location also varied between trials. On days 3-7, the flag was removed from the platform, rendering it hidden, and the curtains were removed, which allowed the mice to now use distal cues to locate the hidden platform. The platform was kept in the middle of the SW quadrant of the maze during days 3-7. On day 8, spatial memory was assayed with a 1min probe trial in which the platform was removed. Reversal training was conducted on days

9-13 with the platform now hidden in the NW quadrant. Spatial memory of the novel location was tested with a 1min probe trial on day 14. Release and platform locations were adapted from previous studies[44].

Fear conditioning

A 3-day delay fear conditioning protocol was employed to test hippocampal-dependent contextual fear memory and amygdala-dependent auditory fear memory. On day 1, the mice were placed in an enclosure (17 cm × 17 cm × 25 cm) with a steel grid floor. This enclosure was located in a sound-attenuating chamber that contained a FireWire camera, light, and speaker. On day 1, the enclosure was outfitted as context A which consisted of 3 plexiglass walls and 1 opaque wall with black and white stripes. 1% acetic acid was placed as the dominant odor, and the house fan was turned on. The enclosure was cleaned with 70% isopropanol between animals. Mice were moved from their home cage to a transfer cage with no bedding and after 15-20s were placed in the fear conditioning chamber. After 150s, a tone (30 s, 2.8 kHz, 85 dB) was played and co-terminated with a shock (2 s, 0.7 mA). Mice were removed from the chamber 30 s after the shock. On day 2, contextual fear memory was assayed by placing the mice back in context A for 300 s. On day 3, the mice were brought to the testing room that was now dimly illuminated with red light. The mice were placed in context B, which consisted of an enclosure with 3 solid gray colored walls, 1 plexiglass wall with a circular door, and a red, flat plastic roof. The floor of the enclosure was a white piece of plastic, 0.25% benzaldehyde was the dominant odor, and the enclosure was cleaned between animals with Vimoba. Mice were first moved from their home cage to a circular bucket and then to the testing chamber. After 180 s, the tone from day 1 was sounded for 60 s. Percent time spent freezing (defined as the absence of all movement except for respiration) was measured throughout these experiments and served as an index of fear memory.

Sociability and social novelty

This test was performed as previously described[23]. Briefly, mice were placed in an arena divided into 3 equal-sized compartments by plastic mesh. On day 1, a 5 min sociability trial was conducted. A littermate was placed in the left or right compartment (systematically alternated) and the test subject was placed into the center compartment. The time the test subject spent investigating each compartment (snout within 2 cm of the mesh barrier) was measured and a difference score was computed. On day 2, a 5 min social novelty test was conducted in which a littermate was placed in either the left or right compartment, and a novel animal (C57BL/6J, 3-month-old, male) was placed in the other compartment. The test subject was placed in the center compartment, investigation time was measured, and a difference score, determined by subtracting the time spent investigating the two compartments, was computed.

Direct interaction

This test was adapted from Kogan *et al.*[25]. Under low light (12lux), mice were placed in a standard clean cage and a novel mouse (C57BL/6J, 4-5-week-old, male) was introduced. Activity was monitored for 5 min and scored online for social behavior (anogenital and

nose-to-nose sniffing, following, and allogrooming) initiated by the test subject. After an ITI of 1 hr, the test was run again with either the previously encountered mouse or a novel mouse. The time spent in social interaction during trial 1 was subtracted from the social interaction time during trial 2 to obtain the difference score.

5-trial social memory assay

This test was run as previously described[26,45]. Briefly, subject mice were individually housed for 7 days prior to testing. On the day of testing, the subjects were presented with a 10 week old CD-1 ovariectomized female mouse for 4 successive 1 minute trials. On the fifth trial, a novel stimulus animal was presented.

Buried food test

To ensure palatability of the food, mice were given 1 g reward treats (F05472-1, Bio-Serv) in their home cages one day before testing. All pellets were consumed. The mice were then food deprived for 18 h before the test to improve sensitivity[46]. A treat was hidden under 1.5 cm of standard cage bedding, a mouse was placed in the cage, and the latency to consumption of the treat was recorded.

Olfactory habituation/dishabituation test

This test was run as previously described[46] with the exclusion of the first 3 trials in which a water-soaked cotton swab is presented. A trained observer measured and recorded olfactory investigation of the odorant-soaked cotton swabs.

Statistical Analysis

Prism 6 (GraphPad) was used for statistical analysis and to graph data. Statistical significance was assessed by two-tailed unpaired Student's t-tests, 2-way ANOVA, or 2-way repeated measures (RM) ANOVA where appropriate. Significant main effects or interactions were followed up with multiple comparison testing using Holm-Sidak's correction. Results were considered significant when $P < 0.05$. α was set equal to 0.05 for multiple comparison tests. Sample sizes were chosen based on previous studies. Data met assumptions of statistical tests and variance was similar between groups for all metrics measured except for AP duration (Extended Data Table 1), social novelty difference score (Fig. 4b), and direct interaction difference score (Fig. 4c).

Acknowledgements

We thank T.R. Reardon for providing the rabies virus and Justine Kupferman and Franklin Lema for experimental assistance. We thank Christine Denny, Zoe Donaldson, René Hen, Josh Gordon, Jayeeta Basu, and Marco Russo for helpful discussions and comments on the manuscript. This work was supported by a Ruth L. Kirschstein F30 NRSA from the NIMH (F.L.H.) and the Howard Hughes Medical Institute (S.A.S.).

References

1. Squire LR, Wixted JT. The cognitive neuroscience of human memory since H.M. Annu. Rev. Neurosci. 2011; 34:259–88. [PubMed: 21456960]

2. van Strien NM, Cappaert NL, Witter MP. The anatomy of memory: an interactive overview of the parahippocampal-hippocampal network. Nat. Rev. Neurosci. 2009; 10:272–282. [PubMed: 19300446]

3. Suh J, Rivest AJ, Nakashiba T, Tominaga T, Tonegawa S. Entorhinal cortex layer III input to the hippocampus is crucial for temporal association memory. Science. 2011; 334:1415–20. [PubMed: 22052975]

4. Nakashiba T, et al. Young dentate granule cells mediate pattern separation, whereas old granule cells facilitate pattern completion. Cell. 2012; 149:188–201. [PubMed: 22365813]

5. Nakashiba T, Young JZ, McHugh TJ, Buhl DL, Tonegawa S. Transgenic inhibition of synaptic transmission reveals role of CA3 output in hippocampal learning. Science. 2008; 319:1260–4. [PubMed: 18218862]

6. Tsien JZ, Huerta PT, Tonegawa S. The essential role of hippocampal CA1 NMDA receptor-dependent synaptic plasticity in spatial memory. Cell. 1996; 87:1327–38. [PubMed: 8980238]

7. Chevaleyre V, Siegelbaum SA. Strong CA2 pyramidal neuron synapses define a powerful disynaptic cortico-hippocampal loop. Neuron. 2010; 66:560–72. [PubMed: 20510860]

8. Lorente de Nó R. Studies on the structure of the cerebral cortex II. Continuation of the study of the ammonic system. J. Psychol. Neurol. 1934; 46:113–177.

9. Franklin, K.; Paxinos, G. The Mouse Brain in Stereotaxic Coordinates. Academic Press; 2007.

10. Lein ES, Callaway EM, Albright TD, Gage FH. Redefining the boundaries of the hippocampal CA2 subfield in the mouse using gene expression and 3-dimensional reconstruction. J. Comp. Neurol. 2005; 485:1–10. [PubMed: 15776443]

11. Fanselow MS, Dong HW. Are the dorsal and ventral hippocampus functionally distinct structures? Neuron. 2010; 65:7–19. [PubMed: 20152109]

12. Lee SE, et al. RGS14 is a natural suppressor of both synaptic plasticity in CA2 neurons and hippocampal-based learning and memory. Proc. Natl. Acad. Sci. USA. 2010; 107:16994–8. [PubMed: 20837545]

13. Cui Z, Gerfen CR, Young WS 3rd. Hypothalamic and other connections with dorsal CA2 area of the mouse hippocampus. J. Comp. Neurol. 2013; 521:1844–66. [PubMed: 23172108]

14. Kohara K, et al. Cell type-specific genetic and optogenetic tools reveal hippocampal CA2 circuits. Nat. Neurosci. 2013 doi: 10.1038/nn.3614.

15. Wall NR, De La Parra M, Callaway EM, Kreitzer AC. Differential Innervation of Direct- and Indirect-Pathway Striatal Projection Neurons. Neuron. 2013; 79:347–60. [PubMed: 23810541]

16. Rowland DC, et al. Transgenically targeted rabies virus demonstrates a major monosynaptic projection from hippocampal area CA2 to medial entorhinal layer II neurons. J. Neurosci. 2013; 33:14889–98. [PubMed: 24027288]

17. Boyden ES, Zhang F, Bamberg E, Nagel G, Deisseroth K. Millisecond-timescale, genetically targeted optical control of neural activity. Nat. Neurosci. 2005; 8:1263–8. [PubMed: 16116447]

18. Hargreaves EL, Rao G, Lee I, Knierim JJ. Major dissociation between medial and lateral entorhinal input to dorsal hippocampus. Science. 2005; 308:1792–4. [PubMed: 15961670]

19. Hensler JG. Serotonergic modulation of the limbic system. Neurosci. Biobehav. Rev. 2006; 30:203–14. [PubMed: 16157378]

20. Pan WX, McNaughton N. The supramammillary area: its organization, functions and relationship to the hippocampus. Prog. Neurobiol. 2004; 74:127–66. [PubMed: 15556285]

21. Young WS, Li J, Wersinger SR, Palkovits M. The vasopressin 1b receptor is prominent in the hippocampal area CA2 where it is unaffected by restraint stress or adrenalectomy. Neuroscience. 2006; 143:1031–9. [PubMed: 17027167]

22. Wersinger SR, Ginns EI, O'Carroll AM, Lolait SJ, Young WS 3rd. Vasopressin V1b receptor knockout reduces aggressive behavior in male mice. Mol. Psychiatry. 2002; 7:975–84. [PubMed: 12399951]

23. DeVito LM, et al. Vasopressin 1b receptor knock-out impairs memory for temporal order. J. Neurosci. 2009; 29:2676–83. [PubMed: 19261862]

24. Stevenson EL, Caldwell HK. The vasopressin 1b receptor and the neural regulation of social behavior. Horm. Behav. 2012; 61:277–82. [PubMed: 22178035]

25. Kogan JH, Frankland PW, Silva AJ. Long-term memory underlying hippocampus- dependent social recognition in mice. Hippocampus. 2000; 10:47–56. [PubMed: 10706216]
26. Ferguson JN, et al. Social amnesia in mice lacking the oxytocin gene. Nat. Genet. 2000; 25:284–8. [PubMed: 10888874]
27. Brennan PA, Zufall F. Pheromonal communication in vertebrates. Nature. 2006; 444:308–315. [PubMed: 17108955]
28. Corkin S. What's new with the amnesic patient H.M.? Nat. Rev. Neurosci. 2002; 2:153–60. [PubMed: 11836523]
29. Benes FM, Kwok EW, Vincent SL, Todtenkopf MS. A reduction of nonpyramidal cells in sector CA2 of schizophrenics and manic depressives. Biol. Psychiatry. 1998; 44:88–97. [PubMed: 9646890]
30. Meyer-Lindenberg A, Domes G, Kirsch P, Heinrichs M. Oxytocin and vasopressin in the human brain: social neuropeptides for translational medicine. Nat. Rev. Neurosci. 2011; 12:524–38. [PubMed: 21852800]
31. Heintz, N. GENSAT Brain Atlas of gene expression in EGFP Transgenic Mice. 2003. http://www.gensat.org
32. Lein, ES. ISH Data :: Allen Brain Atlas: Mouse Brain. 2007. http://mouse.brain-map.org/
33. de Jong, PJ. BAC Clones Distribution Center – BACPAC Resources Center; 2000. https://bacpac.chori.org/
34. Warming S, Costantino N, Court DL, Jenkins NA, Copeland NG. Simple and highly efficient BAC recombineering using galK selection. Nucleic Acids Res. 2005; 33:e36. [PubMed: 15731329]
35. Gong S, et al. Targeting Cre recombinase to specific neuron populations with bacterial artificial chromosome constructs. J. Neurosci. 2007; 27:9817–23. [PubMed: 17855595]
36. Madisen L, et al. A robust and high-throughput Cre reporting and characterization system for the whole mouse brain. Nat. Neurosci. 2010; 13:133–40. [PubMed: 20023653]
37. Wickersham IR, Sullivan HA, Seung HS. Production of glycoprotein-deleted rabies viruses for monosynaptic tracing and high-level gene expression in neurons. Nat. Protoc. 2010; 5:595–606. [PubMed: 20203674]
38. Watabe-Uchida M, Zhu L, Ogawa SK, Vamanrao A, Uchida N. Whole-brain mapping of direct inputs to midbrain dopamine neurons. Neuron. 2012; 74:858–73. [PubMed: 22681690]
39. Yamamoto M, et al. Reversible suppression of glutamatergic neurotransmission of cerebellar granule cells in vivo by genetically manipulated expression of tetanus neurotoxin light chain. J. Neurosci. 2003; 23:6759–67. [PubMed: 12890769]
40. Jiao Y, et al. A simple and sensitive antigen retrieval method for free-floating and slide- mounted tissue sections. J. Neurosci. Methods. 1999; 93:149–62. [PubMed: 10634500]
41. Boulanger LM, et al. Cellular and molecular characterization of a brain-enriched protein tyrosine phosphatase. J. Neurosci. 1995; 15:1532–44. [PubMed: 7869116]
42. Takeda K, et al. WFS1 (Wolfram syndrome 1) gene product: predominant subcellular localization to endoplasmic reticulum in cultured cells and neuronal expression in rat brain. Hum. Mol. Genet. 2001; 10:477–84. [PubMed: 11181571]
43. Rasband, WS. Image J. 1997. http://imagej.nih.gov/ij/
44. Vorhees CV, Williams MT. Morris water maze: procedures for assessing spatial and related forms of learning and memory. Nat. Protoc. 2006; 1:848–58. [PubMed: 17406317]
45. Bielsky IF, Hu S, Szegda KL, Westphal H, Young LJ. Profound Impairment in Social Recognition and Reduction in Anxiety-Like Behavior in Vasopressin V1a Receptor Knockout Mice. Neuropsychopharmacology. 2004; 29:483–93. [PubMed: 14647484]
46. Yang M, Crawley JN. Simple behavioral assessment of mouse olfaction. Curr. Protoc. Neurosci. 2009; 84:8.24.1–8.24.12.

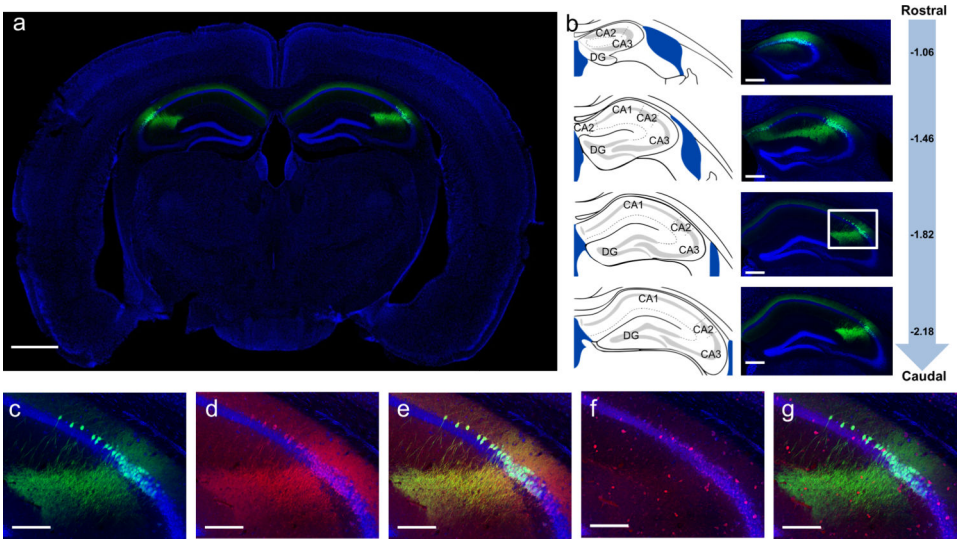

Figure 1. Genetic targeting of the CA2 subfield using the *Amigo2-Cre* mouse line

a, Bilateral hippocampal injection (n = 64) of Cre-dependent YFP AAV in *Amigo2-Cre* mice resulted in specific expression of YFP (green) in CA2 PNs. **b**, Extent of transduction. Left, adapted reference atlas images[9]. Center, YFP expression. Right, mm from bregma along rostrocaudal axis. **c-g**, Magnified images of boxed area in (**b**). **c**, YFP (green). **d**, RGS14 staining (red, n = 4). **e**, Merge of (**c**) and (**d**) showing YFP and RGS14 overlap. **f**, GABA staining (red, n = 3). **g**, merge of (**c**) and (**f**) showing no GABA and YFP overlap. Panels show coronal sections with Nissl counterstain (blue). Scale bars, 1000 μm, 400 μm, 200 μm in (**a**), (**b**), (**c-g**), respectively.

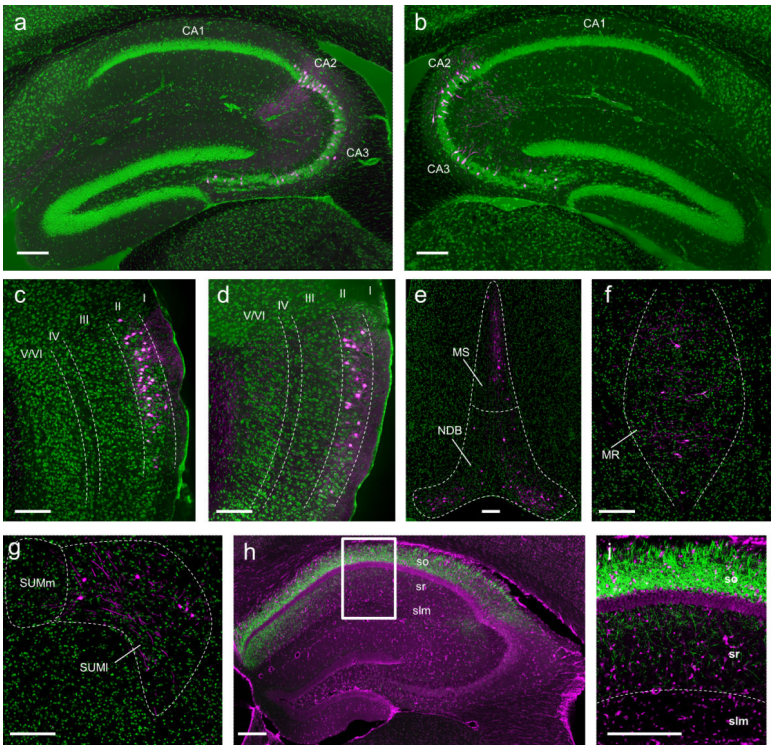

Figure 2. Genetically targeted tracing of the CA2 circuit

a-g, Monosynaptic inputs to CA2 revealed with pseudotyped rabies virus (*n* = 8). Cells labeled with rabies (magenta); Nissl (green). Sagittal sections (**a-d)** and coronal sections (**e-g**). **a, b**, Labeled neurons in CA2 and CA3 ipsilateral (**a**) and contralateral (**b**) to hemisphere of rabies virus injection. Rabies labeling shows monosynaptic inputs from lateral EC (**c**), medial EC (**d**), medial septum (MS), nucleus of the diagonal band (NDB) (**e**), median raphe (MR) (**f**), and lateral supramammillary nucleus (SUMl) (**g**). Fluorescent processes in (**c,d**) may represent dendritic or axonal labeling. **h, i**, Output of CA2 revealed by axonal YFP signal (green, *n* = 6). Nissl stain (magenta). **i**, Magnification of boxed area in (**h**). Note strong labeling of CA2 projections to SO and SR of CA1. Scale bars, 200 μm. slm, stratum lacunosum-moleculare.

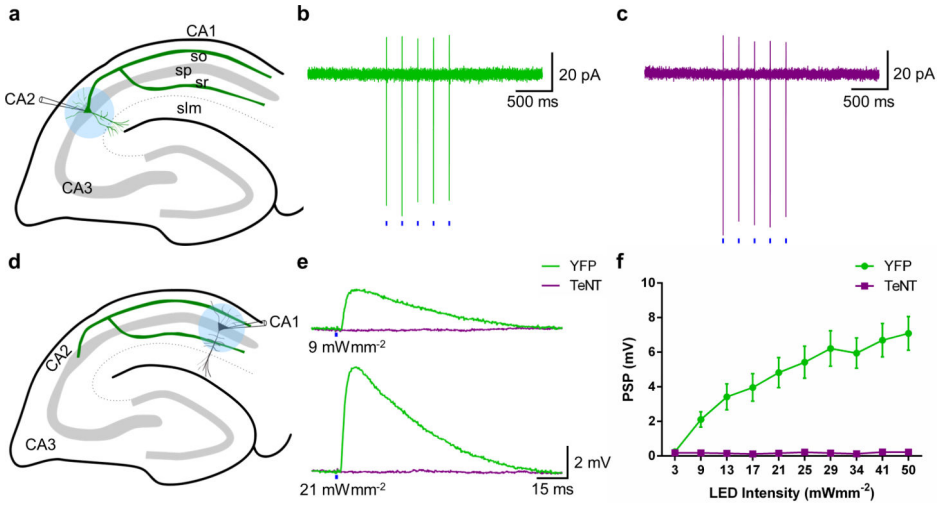

Figure 3. Electrophysiological verification of CA2 inactivation with tetanus toxin

a, Experimental setup for photostimulation of CA2 PNs. **b, c**, Action currents recorded from CA2 PNs expressing YFP and ChR2 (n = 6) (**b**) or TeNT and ChR2 (n = 4) (**c**) in response to five 2-ms blue (470 nm) light pulses (blue bars). **d**, Experimental setup for current-clamp recordings of photostimulated PSPs in CA1 PNs. **e**, PSPs recorded when YFP (n = 14, green) or TeNT (n = 14, magenta) was co-expressed with ChR2 in CA2 PNs. **f**, Mean input-output curve of PSP as function of light intensity when YFP or TeNT was co-expressed with ChR2 in CA2 PNs. Data show mean ± s.e.m.

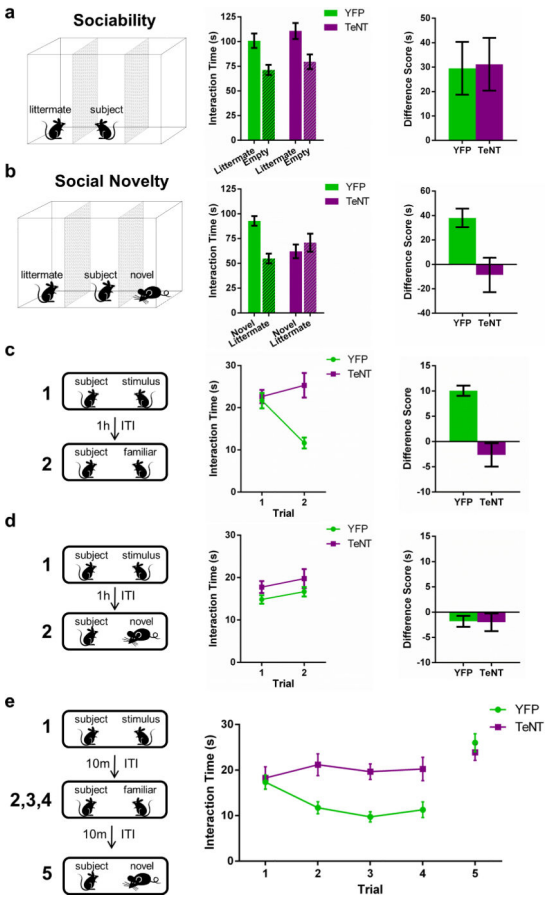

Figure 4. Inactivation of CA2 pyramidal neurons abolishes social memory

a, Left, sociability test. Middle, Both YFP (n = 11) and TeNT (n = 13) groups preferred the chamber with a littermate (YFP, P = 0.0083; TeNT, P = 0.0055; multiplicity adjusted P values) and did not differ significantly (two-way ANOVA: Treatment × Chamber F(1,44) = 0.013, P = 0.91; Treatment F(1,44) = 1.566, P = 0.22; Chamber F(1,44) = 17.49, P = 0.0001). Right, The groups had similar interaction time difference scores (littermate – empty) (P = 0.9154, two-tailed t-test). **b**, Left, social novelty test. Middle, The YFP, but not the TeNT, group preferred the novel animal (YFP, P = 0.0012; TeNT, P = 0.3593; multiplicity adjusted P values); the groups differed significantly (two-way ANOVA: Treatment × Chamber F(1,44) = 11.25, P = 0.0016). Right, TeNT group showed a significantly lower difference score (novel – littermate) than the YFP group (P = 0.0109, two-tailed t-test). **c**, **d**, Left, direct interaction test using the same (**c**) or different (**d**) stimulus animals in two trials. **c**, Middle, The YFP, but not the TeNT, mice displayed decreased investigation of a familiar stimulus mouse during trial 2 (YFP, n = 15, P < 0.0001; TeNT, n = 16, P = 0.1499; multiplicity adjusted P values); the two groups differed significantly (two-way RM ANOVA: Treatment × Trial F(1,29) = 24.23, P < 0.0001). Right, difference score (trial 1 – trial 2) of TeNT group was less than that of YFP group (P < 0.0001; two-tailed t-test). **d**, Middle, The two groups explored the two different stimulus animals for similar amounts of time (two-way RM ANOVA: Treatment × Trial F(1,29) = 0.0068, P = 0.93; Treatment F(1,29) = 2.405, P = 0.13; Trial F(1,29) = 3.278, P = 0.0806), with similar

difference scores (Right, P = 0.93, two-tailed t-test). **e**, 5-trial social memory assay. The YFP group (*n* = 15), but not the TeNT group (*n* = 14), habituated to repeated presentation of the same stimulus mouse (trials 1-4) and dishabituated to the novel mouse (trial 5). Two-way RM ANOVA confirmed a significant difference between the groups (Treatment × Trial $F(4,108) = 7.26$, $P < 0.0001$; Treatment $F(1,27) = 7.86$, $P = 0.009$; Trial $F(4,108) = 15.41$, $P < 0.0001$). Data show mean ± s.e.m.

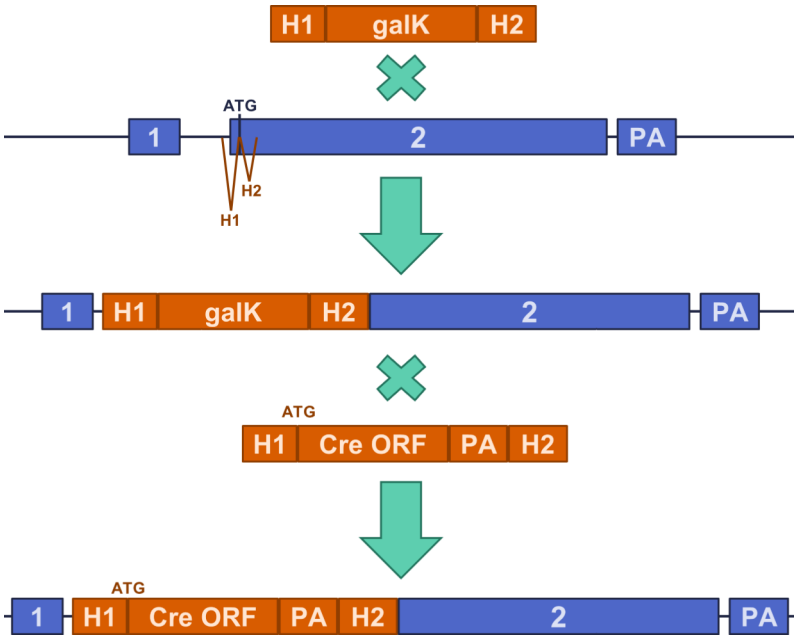

Extended Data Figure 1. Generation of *Amigo2-Cre* mouse line

λ Red-mediated homologous recombination with galK positive and negative selection was used to make seamless changes to the bacterial artificial chromosome (BAC). PCR cassettes shown in orange, and *Amigo2* locus shown in blue. The PCR cassette contained two homology arms (H1, 58nt; H2, 62nt) that flanked the galactose kinase (galK) cassette. The homology arms flanked the *Amigo2* start codon. Recombination followed by positive selection was used to obtain the galK integrate. Recombination of the modified BAC with a PCR cassette containing the Cre open reading frame (ORF) and polyA (PA) flanked by the same homology arms yielded the final BAC used to generate the transgenic line.

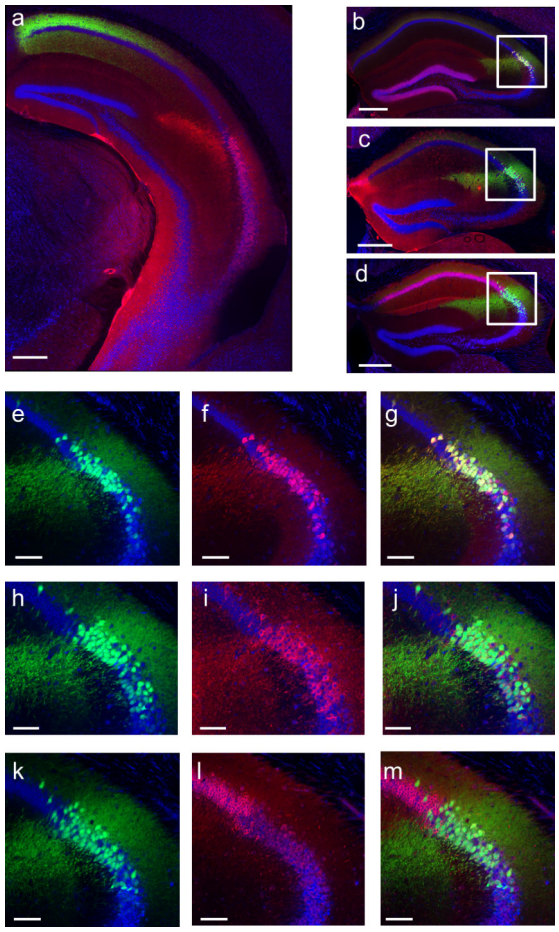

Extended Data Figure 2. *Amigo2-Cre* mice express Cre in a genetically defined population of CA2 PNs

Coronal sections of hippocampus from *Amigo2-Cre* mice injected in dorsal hippocampus with a Cre-dependent AAV to express YFP (shown in green) in CA2. **a**, Coronal section of ventral hippocampus (~2.8 mm caudal to bregma, see Figure 54 of Franklin & Paxinos[9] for reference image) showing CA2 axons (green) from dorsal CA2. Note absence of YFP in ventral CA2 neurons (RGS14 stain in red). **b**, 97.22 ± 0.46% of YFP^+ cells (n = 4 mice, 2948 cells) express the CA2 marker PCP4 (red). **c**, 98.45 ± 0.33% of YFP^+ cells (n = 4 mice, 2870 cells) express the CA2 marker STEP (red). **d**, Nearly no YFP^+ cells (0.17 ± 0.13%; n = 4 mice, 2870 cells) express the CA1 marker WFS1 (red). **e-f**, Magnification of boxed area in **(b)** showing YFP signal (**e**) PCP4 staining (**f**) and a merge of the two (**g**). **h-j**, Magnification of boxed area in (**c**) showing YFP signal (**h**) STEP staining (**i**) and a merge of the two (**j**). **k-m**, Magnification of boxed area in (**d**) showing YFP signal (**k**) WFS1 staining (**l**) and a merge of the two (**m**). Nissl stain shown in blue. Scale bars, 400 μm (**a-d**) and 100 μm (**e-m**).

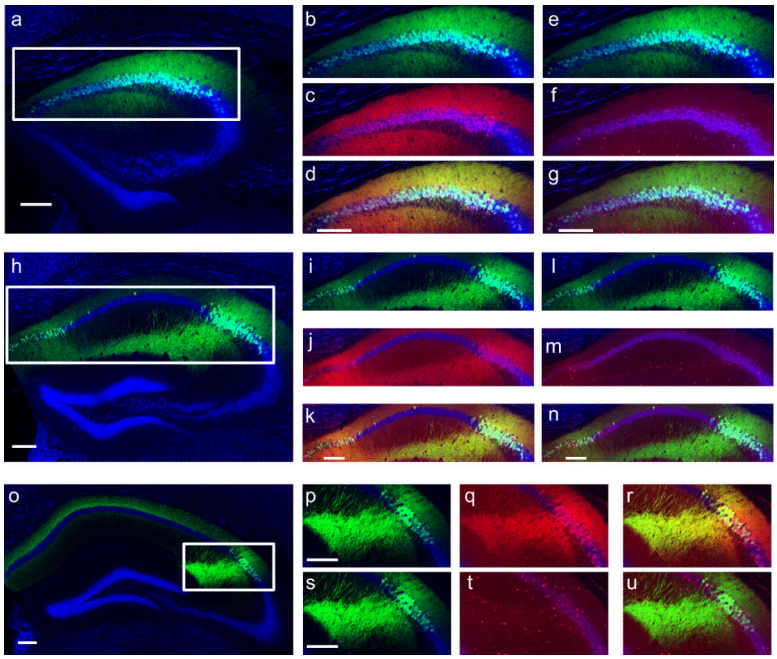

Extended Data Figure 3. *Amigo2-Cre* mice express Cre in RGS14^{+} CA2 PNs but not in GABAergic inhibitory neurons

Cre^{+} neurons expressing YFP (shown in green) co-label with RGS14 staining (shown in red), but do not co-label with GABA staining (shown in red in separate images). **a**, Reproduction of section −1.06 mm shown in Fig. 1b. **b, e**, Magnification of area boxed in (**a**). **c**, RGS14 staining of section shown in (**b**). **d**, Merge of (**b, c**) demonstrating YFP and RGS14 co-labeling. **f**, GABA staining of section shown in (**e**). **g**, Merge of (**e, f**) showing no overlap of GABA and YFP. **h**, Reproduction of section −1.46 mm shown in Fig. 1b. **i, l**, Magnification of area boxed in (**h**). **j**, RGS14 staining of section shown in (**i**). **k**, Merge of (**i**, **j**) demonstrating YFP and RGS14 co-labeling. **m**, GABA staining of section shown in (**l**). **n**, Merge of (**l, m**) showing no overlap of GABA and YFP. **o**, Reproduction of section −2.18mm shown in Fig. 1b. **p, s**, Magnification of area boxed in (**o**). **q**, RGS14 staining of section shown in (**p**). **r**, Merge of (**p, q**) demonstrating YFP and RGS14 co-labeling. **t**, GABA staining of section shown in (**s**). **u**, Merge of (**s, t**) showing no overlap of GABA and YFP. Scale bars, 200 μm. Nissl stain shown in blue.

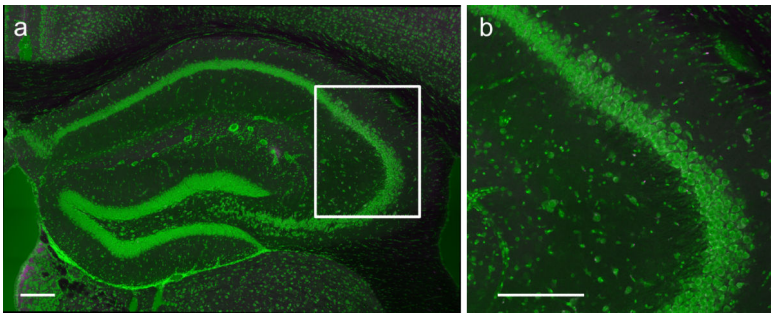

Extended Data Figure 4. Specificity of the pseudotyped rabies virus

a, b, No labeled cells were observed (*n* = 3 mice) following injection of the (EnvA)SAD-ΔG-mCherry virus when TVA was not expressed in CA2. **b**, Magnification of boxed area in (**a**). Rabies labeling would have appeared in magenta; Nissl stain shown in green. Scale bars, 200 μm.

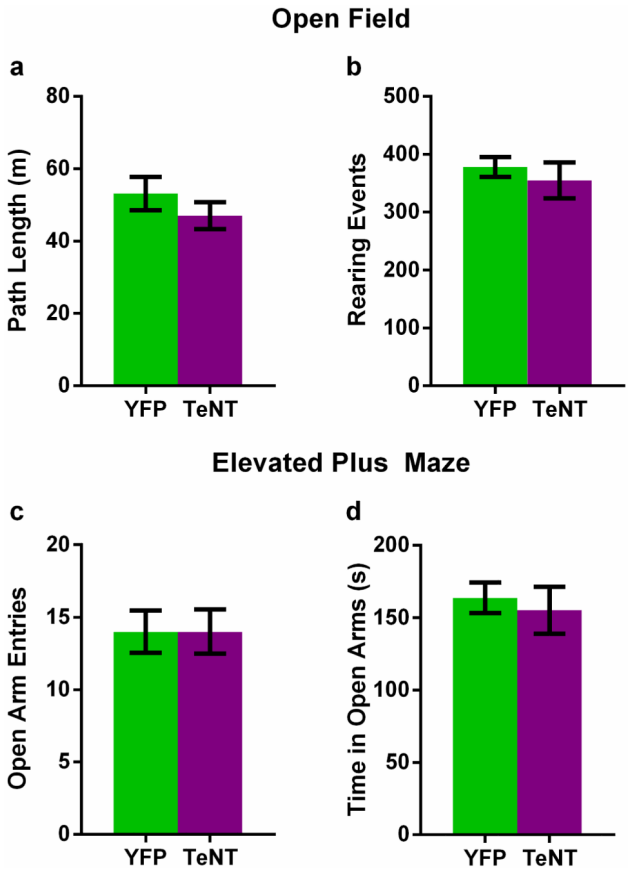

Extended Data Figure 5. Inactivation of CA2 does not alter locomotor activity or anxiety-like behavior

a, There was no significant difference (P = 0.31, two-tailed unpaired t-test) between CA2-YFP and CA2-TeNT groups in the distance traveled in the open field (OF) test (YFP, 53.14 ± 4.62m, *n* = 8; TeNT, 47.04 ± 3.70m, *n* = 10). **b**, There was also no significant difference (P = 0.55, two-tailed unpaired t-test) between the groups in the number of rearing events recorded during the OF session (YFP, 378.0 ± 17.36, *n* = 8; TeNT, 354.7 ± 30.99, *n* = 10). **c, d**, Inactivation of CA2 did not alter anxiety-like behavior measured in the elevated plus maze (EPM). The number of open arm entries was not significantly different (P > 0.99, two-tailed unpaired t-test) between the groups (YFP, 14.00 ± 1.46, *n* = 8; TeNT, 14.00 ± 1.54, *n* = 10). Additionally, the time spent in the open arms (YFP, 163.7 ± 10.43s *n* = 8; TeNT, 155.1 ± 16.38s *n* = 10) did not differ significantly (P = 0.68, two-tailed unpaired t-test) between the groups. Results are presented as mean ± s.e.m.

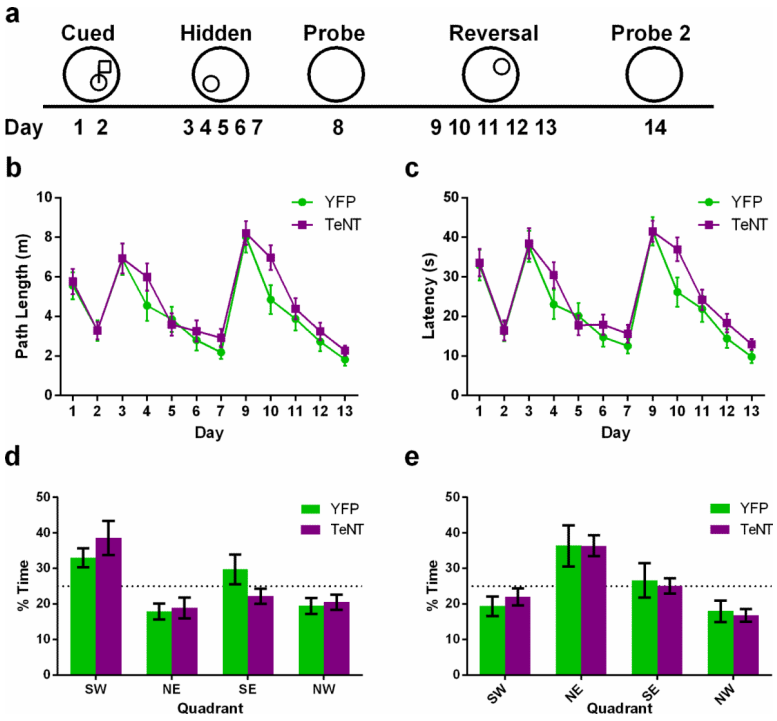

Extended Data Figure 6. Spatial learning and memory assayed with the Morris water maze (MWM) task is unaltered by CA2 inactivation

a, Schema of the experimental design. On days 1 and 2, mice were trained to find a platform with a visible flag. On days 3-7, mice were trained to find a hidden platform located in the SW quadrant of the water maze. Spatial memory was assayed on day 8 with the platform removed. Reversal training was conducted on days 9-13 with the platform now hidden in the NW quadrant. Spatial memory of the novel location was tested on day 14. **b**, Path length to the platform was not altered significantly by CA2 inactivation (two-way repeated measures ANOVA: Treatment × Time $F(11,770) = 0.67$, $P = 0.77$; Time $F(11,770) = 21.87$, $P < 0.0001$; Treatment $F(1,70) = 2.85$, $P = 0.10$). **c**, Latency to find the platform did not differ significantly between the two groups (two-way repeated measures ANOVA: Treatment × Time $F(11,770) = 0.78$, $P = 0.66$; Time $F(11,770) = 25.23$, $P < 0.0001$; Treatment $F(1,70) = 2.84$, $P = 0.10$). YFP, $n = 8$; TeNT, $n = 10$. **d**, Spatial memory during the probe trial was unaffected by CA2 inactivation. The percent of time spent in the target quadrant (YFP, 33.00 ± 2.66%; TeNT, 38.6 ± 4.79%) was not significantly different between the two groups ($P = 0.36$, two-tailed unpaired t-test). **e**, Spatial memory following reversal training was unaffected by CA2 inactivation. There was no significant difference between the groups in percent time spent in the target quadrant during the probe trial following reversal training (YFP, 36.38 ± 5.75%; TeNT, 36.40 ± 2.92%; $P > 0.99$, two-tailed unpaired t-test). Results are presented as mean ± s.e.m.

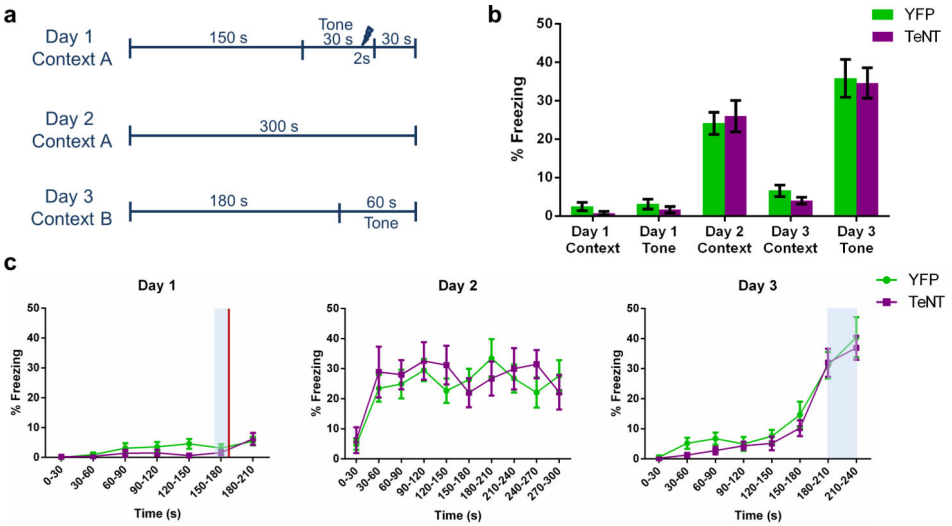

Extended Data Figure 7. Contextual fear conditioning memory and auditory fear conditioning memory are unaffected by inactivation of CA2

a, Schema of the experimental design. Delay fear conditioning was employed to test hippocampal-dependent contextual fear memory and amygdala-dependent auditory fear memory. **b**, There was no significant difference in percent freezing between the groups (two-way repeated measures ANOVA: Treatment × Day $F(4,68) = 0.31$, $P = 0.87$; Treatment $F(1,17) = 0.13$, $P = 0.73$; Day $F(4,68) = 100.8$, $P < 0.0001$; YFP, $n = 11$; TeNT, $n = 8$). Prior to training on day 1, neither group exhibited a fear response to context A (YFP, 2.45 ± 1.06%; TeNT, 0.75 ± 0.49%) or to the tone (YFP, 3.09 ± 1.31%; TeNT, 1.63 ± 0.84%). On day 2 after training, robust fear responses to context A were measured in both groups (YFP, 24.09 ± 2.88%; TeNT, 26.00 ± 4.10%). Both groups exhibited low levels of freezing on day 3 in novel context B (YFP, 6.55 ± 1.52%; TeNT, 4.00 ± 0.87%) demonstrating context specificity of the fear memory and a lack of fear generalization. Both groups exhibited robust freezing to the tone on day 3 (YFP, 35.82 ± 4.93%; TeNT, 34.63 ± 3.96%), demonstrating intact auditory fear memory. **c**, Freezing data plotted in 30s bins. Shaded areas represent tone presentation. Red line represents shock delivery. Left, two-way repeated measures ANOVA revealed no significant difference between groups in freezing on day 1 (Treatment × Time $F(6,102) = 1.135$, $P = 0.3474$; Treatment $F(1,17) = 1.116$, $P = 0.3056$; Time $F(6,102) = 6.348$, $P < 0.0001$). Middle, two-way repeated measures ANOVA revealed no significant difference between groups in freezing on day 2 (Treatment × Time $F(9,153) = 0.9741$, $P = 0.4637$; Treatment $F(1,17) = 0.1326$, $P = 0.7203$; Time $F(9,153) = 6.335$, $P < 0.0001$). Right, two-way repeated measures ANOVA revealed no significant difference between groups in freezing on day 3 (Treatment × Time $F(7,119) = 0.2490$, $P = 0.9716$; Treatment $F(1,17) = 0.6517$, $P = 0.4307$; Time $F(7,119) = 50.87$, $P < 0.0001$). Results are presented as mean ± s.e.m.

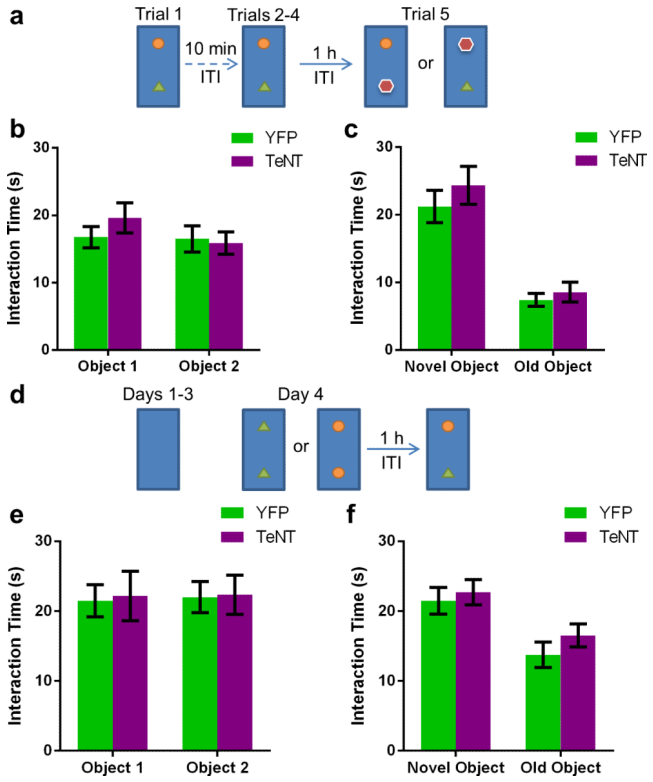

Extended Data Figure 8. Object recognition memory and preference for novelty is preserved in CA2-TeNT animals

a, Schema of the experimental design for the novel object recognition task. **b**, The groups did not differ significantly in exploration of object 1 (YFP, 16.75 ± 1.57s; TeNT, 19.60 ± 2.24s) or object 2 (YFP, 16.50 ± 1.97s; TeNT, 15.90 ± 1.66s) averaged over the course of the first 4 trials (two-way ANOVA: Treatment × Object $F(1,32) = 0.80$, $P = 0.38$; Object $F(1,32) = 1.05$, $P = 0.31$; Treatment $F(1,32) = 0.34$, $P = 0.56$; YFP, $n = 8$; TeNT, $n = 10$). **c**, Both groups explored the novel object (YFP, 21.23 ± 2.37s; TeNT, 24.37 ± 2.81s) more than the familiar object (YFP, 7.41 ± 0.92s; TeNT, 8.57 ± 1.48s). Statistical analysis revealed a significant effect of object, but not CA2 inactivation or interaction of the two (two-way ANOVA: Treatment × Object $F(1,28) = 0.22$, $P = 0.64$; Object $F(1,28) = 48.46$, $P < 0.0001$; Treatment $F(1,28) = 1.02$, $P = 0.32$). Multiple comparison testing revealed a significant difference between exploration of the novel object compared to exploration of the old object for both the YFP group ($P = 0.0002$) and the TeNT group ($P < 0.0001$). **d**, Schema of the experimental design for another variation of the novel object recognition task. **e**, The groups did not differ significantly in time spent exploring object 1 (YFP, 21.50 ± 2.31s; TeNT, 22.18 ± 3.57s) or object 2 (YFP, 22.02 ± 2.23s; TeNT, 22.36 ± 2.81s) during trial 1 of day 4 (two-way ANOVA: Treatment × Object $F(1,44) = 0.004$, $P = 0.95$; Object $F(1,44) = 0.02$, $P = 0.90$; Treatment $F(1,44) = 0.03$, $P = 0.85$; YFP, $n = 12$; TeNT, $n = 12$). **f**, Both groups explored the novel object (YFP, 21.49 ± 1.91s; TeNT, 22.73 ± 1.82s) more than the familiar object (YFP, 13.74 ± 1.83s; TeNT, 16.53 ± 1.64s). Statistical analysis revealed a significant effect of object, but not CA2 inactivation or interaction of the two (two-way ANOVA: Treatment × Object $F(1,44) = 0.18$, $P = 0.67$; Object $F(1,44) = 15.02$, $P = 0.0004$; Treatment $F(1,44) = 1.25$, $P = 0.27$). Multiple comparison testing revealed a significant difference

between exploration of the novel object compared to exploration of the old object for both the YFP group (P = 0.008) and the TeNT group (P = 0.02). Results are presented as mean ± s.e.m.

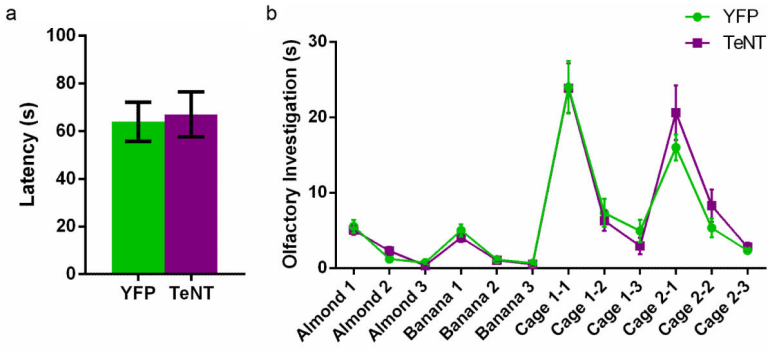

Extended Data Figure 9. Olfaction is unaffected by CA2 inactivation

a, There was no significant difference between the groups in latency to find a buried food pellet (YFP, 63.93 ± 8.22s, *n* = 15; TeNT, 67.06 ± 9.42s *n* = 16; P = 0.81, two-tailed unpaired t-test). **b**, There was no significant difference between the groups (YFP, *n* = 15; TeNT, *n* = 14) in performance on the olfactory habituation/dishabituation task (two-way repeated measures ANOVA: Treatment x Trial $F(11,297) = 0.933$, P = 0.51; Treatment $F(1,27) = 0.08$, P = 0.78; Trial $F(11,297) = 60.21$, $P < 0.0001$). Results are presented as mean ± s.e.m.

Extended Data Table 1

Electrophysiological properties of Cre$^+$ neurons

The electrophysiological properties of Cre$^+$ neurons (Column 1) closely matched the properties previously reported[7] for CA2 neurons and significantly differed from the properties of CA1 neurons (Column 2). Two-tailed unpaired t-tests were used to assess significant differences between the neuronal populations. The P values are shown in Column 3. Whole-cell recordings of Cre$^+$ (n = 5) and CA1 (n = 9) neurons were conducted to measure input resistance, capacitance, resting potential, action potential (AP) amplitude, AP duration, and sag. Input resistance and capacitance were measured with a −5 mV pulse. The AP amplitude and duration were measured during a 500 ms depolarizing pulse and the sag resulting from activation of I_h was measured during a 500 ms hyper-polarization from −70 to −100mV. Smaller sag in Cre$^+$ neurons compared to that previously reported[7] is likely due to differences in extent of whole-cell dialysis resulting from differences in recording protocols.

	Cre$^+$ neurons	CA1	P value
Input Resistance (MΩ)	68.3 ± 3.03	90.0 ± 6.65	0.039
Capacitance (pF)	296.0 ± 18.68	140.7 ± 8.02	< 0.0001
Resting Potential (mV)	−76.3 ± 0.63	−72.8 ± 0.92	0.024
AP Amplitude (mV)	90.81 ± 2.17	99.15 ± 1.36	0.007
AP Duration (ms)	0.83 ± 0.02	1.06 ± 0.06	0.031
Sag (mV)	1.92 ± 0.50	7.55 ± 0.85	0.0006